

The impact of different voltage application modes on biodegradation of chloramphenicol and shift of microbial community structure

Yifan Liu^{1,2,#}, Qiongfang Zhang^{1,2,#}, Ainiwaer Sidike³, Nuerla Ailijiang (✉)^{1,2}, Anwar Mamat⁴, Guangxiao Zhang^{1,2}, Miao Pu^{1,2}, Wenhui Cheng^{1,2}, Zhengtao Pang^{1,2}

¹ Key Laboratory of Oasis Ecology of Education Ministry, College of Ecology and Environment, Xinjiang University, Urumqi 830017, China

² Xinjiang Jinghe Observation and Research Station of Temperate Desert Ecosystem, Ministry of Education, Urumqi 830017, China

³ School of Geographical Sciences, Xinjiang University, Urumqi 830017, China

⁴ School of Chemical Engineering and Technology, Xinjiang University, Urumqi 830017, China

HIGHLIGHTS

- Presented coupled system enhanced biodegradation of antibiotic chloramphenicol.
- HRT and electrical stimulation modes were key influencing factors.
- Electrical stimulation had little effect on the chloramphenicol metabolic pathway.
- Microbial community structure varied with the voltage application mode.

ARTICLE INFO

Article history:

Received 16 November 2021

Revised 16 April 2022

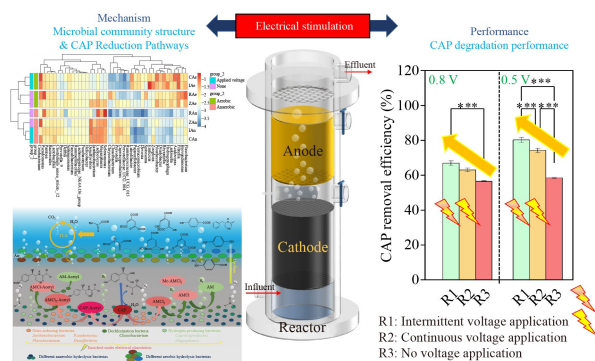
Accepted 18 April 2022

Available online 20 May 2022

Keywords:

Electrical stimulation
Biodegradation
Microbial community
Chloramphenicol

GRAPHIC ABSTRACT



ABSTRACT

Exoelectrogenic biofilms have received considerable attention for their ability to enhance electron transfer between contaminants and electrodes in bioelectrochemical systems. In this study, we constructed anaerobic-aerobic-coupled upflow bioelectrochemical reactors (AO-UBERs) with different voltage application modes, voltages and hydraulic retention times (HRTs). In addition, we evaluated their capacity to remove chloramphenicol (CAP). AO-UBER can effectively mineralize CAP and its metabolites through electrical stimulation when an appropriate voltage is applied. The CAP removal efficiencies were $\sim 81.1\% \pm 6.1\%$ (intermittent voltage application mode) and $75.2\% \pm 4.6\%$ (continuous voltage application mode) under 0.5 V supply voltage, which were $\sim 21.5\%$ and 15.6% greater than those in the control system without voltage applied, respectively. The removal efficiency is mainly attributed to the anaerobic chamber. High-throughput sequencing combined with catabolic pathway analysis indicated that electrical stimulation selectively enriched *Megasphaera*, *Janthinobacterium*, *Pseudomonas*, *Emticicia*, *Zoogloea*, *Cloacibacterium* and *Cetobacterium*, which are capable of denitrification, dechlorination and benzene ring cleavage, respectively. This study shows that under the intermittent voltage application mode, AO-UBERs are highly promising for treating antibiotic-contaminated wastewater.

© Higher Education Press 2022

✉ Corresponding author
E-mail: aljnel@xju.edu.cn

#These authors contributed to the work equally and should be regarded as co-first authors.

1 Introduction

Chloramphenicol (CAP) is a broad-spectrum antibiotic that has been extensively used in the treatment of bacterial infections in humans and livestock since 1949,

when it was first artificially synthesized on a large scale. Subsequently, it has been frequently detected in sewage and natural waters worldwide (Yang et al., 2021). CAP has adverse health implications for humans. It causes aplastic anemia and is potentially genotoxic and carcinogenic (Xiong et al., 2022). In addition to endangering human health, residual antibiotics in the environment exert intense, but selective, pressure on microbial communities, triggering the dissemination of antibiotic-resistance genes and the evolution of antibiotic-resistant bacteria (Zhao et al., 2021). Although several solutions exist for this issue, including zero-valent iron-based catalytic techniques (Tang et al., 2021), photolysis (Xiong et al., 2022), Fenton reagents (Yang et al., 2021) and advanced oxidation processes (Xue et al., 2021), the consumables and materials of these methods are costly and impractical for broad-scale applications. In contrast to physical and chemical processes, biodegradation is an eco-friendly and energy-efficient approach for CAP removal (Zhao et al., 2021). Unfortunately, the presence of nitro and chlorine substituents in CAP inhibits ribosomal peptide transferase activity and limits CAP removal in conventional wastewater treatment plants (WWTPs). Activated sludge is inhibited by the biological toxicity of CAP, which reduces the efficacy of wastewater treatment in WWTPs (Xue et al., 2021). Thus, there is an urgent need to develop effective and environmentally-friendly methods for CAP degradation.

Exoelectrogenic biofilm technology (EBT) is a persistent contaminant treatment process based on bioelectrochemical systems that catalyze electrons between electrode surfaces and contaminants by applying an electric field (Logan and Rabaey, 2012). EBT has been extensively studied and is considered an energy-efficient and promising technique for facilitating microbial metabolism to degrade various pollutants (Logan et al., 2019; Jiang et al., 2021). EBT can prevent biofilms from being attacked by biotoxic compounds (e.g., heavy metals, sterilants and antibiotics), facilitate nitro reduction and dechlorination and promote the degradation of aromatic hydrocarbons (Jiang et al., 2016; Zhang et al., 2019; Wang et al., 2022). In addition, the treatment efficiency of pollutants is significantly different in various electrical stimulation modes, including continuous and intermittent electrical stimulation modes (Cao et al., 2016; Wu et al., 2016; Ailijiang et al., 2021b). However, there are no data on the decomposition of complex antibiotic compounds upon exposure to different modes of electrical stimulation. Anaerobic-aerobic-coupled upflow bioelectrochemical reactors (AO-UBERs) have outstanding potential for accelerating the aerobic and anaerobic removal of chloro and nitro substituents from refractory organic pollutants (Ailijiang et al., 2021b). However, the mechanism by which electrical stimulation affects CAP decomposition in AO-UBERs remains poorly understood.

In this study, three AO-UBERs were constructed to

accelerate CAP biodegradation. For this purpose, we 1) analyzed the effects of different applied voltages, voltage application modes and hydraulic retention times (HRTs) on the biodegradation of CAP; 2) determined the relative contributions of cathodic and anodic chambers in CAP degradation; and 3) examined the degradation pathway of CAP and microbial community changes in AO-UBERs.

2 Materials and methods

2.1 Reactor configurations

The three pilot reactors were the same as those used in a previous study using an organic glass vessel with a working volume of 675 mL (height, inner diameter and thickness of 43 cm, 5 cm and 5 mm, respectively) (Ailijiang et al., 2021a). The influent was fed from the bottom of the AO-UBER and sequentially passed through the cathode chamber (anaerobic zone), aeration zone, anode chamber (aerobic zone) and overflow zones. All the parts were separated using a titanium mesh. A gas diffuser was installed between the anaerobic and aerobic zones to create an aeration zone (Fig. 1). The primary function of the gas diffuser is to provide a continuous and stable supply of dissolved oxygen for bacteria in the aerobic zone. Carbon felt nubbles (CFNs) with a pre-acclimated aerobic biofilm (10 mm length \times 10 mm width \times 8 mm height) and granular activated carbon (GAC; biofilm carrier) attached to an anaerobic biofilm (2–3 mm in diameter and 3–5 mm in length) were utilized as bioelectrodes.

Thirty CFNs were fixed in the aerobic zone after enrichment with the aerobic biofilms. A total mass of 310 g (wet weight) of GAC was placed on a titanium mesh in the anaerobic zone. Titanium meshes with a diameter of 6 cm were installed in the anaerobic and aerobic zones; the titanium mesh sizes were 2 mm \times 2 mm and 50 mm \times 50 mm, respectively. A 20 mm wide titanium strip was inserted into the two zones to transfer electrons between the direct electric current (DC) supplier (APS3005S-3D, Guorui Antaixin Technology Co., Ltd, Nanjing, China) and the biofilm.

2.2 Adsorption of bacteria into biofilms

Aerobic and anaerobic activated seed sludge used as inocula was obtained from the Hedong and Midong District WWTP (Xinjiang Uygur Autonomous Region, China). The sludge was acclimated using CAP-containing synthetic wastewater (Table S1) for one month. GAC (1200 g, wet weight) was submerged in the acclimated sludge for four weeks (Fig. S1A) and the CFNs were strung together on an iron wire in groups of 20. Subsequently, they were immersed in a 10 L bucket containing domesticated sludge (Fig. S1B), to enable

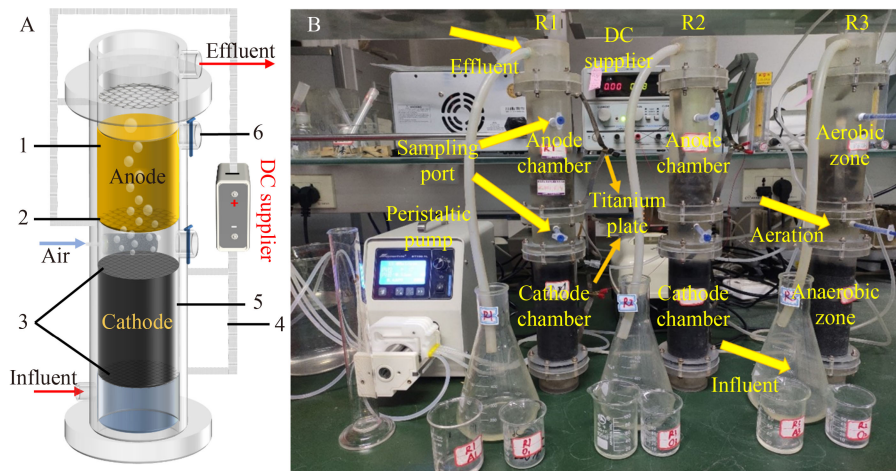


Fig. 1 (A) Schematic diagram of AO-UBER. (B) AO-UBER photos. (1, CFNs; 2, titanium mesh (screen mesh size of 50 mm × 50 mm); 3, titanium mesh (screen mesh size of 2 mm × 2 mm); 4, titanium plate; 5, GACs; and 6, sampling port); (R1: intermittent voltage applied; R2: continuous voltage applied; and R3: control reactor without voltage applied).

sufficient biofilm formation on the carriers.

2.3 Experimental operation

Synthetic simulated CAP wastewater containing CAP (10 mg/L; microbial tolerance concentration in the pre-domestication phase) and glucose (700 mg/L) was used in this study. Ammonium chloride (NH_4Cl) and monopotassium phosphate (KH_2PO_4) were added as the nitrogen and phosphorus sources, respectively, to maintain a COD/N/P ratio of 200/5/1. The mineral solution was added to synthetic wastewater, which contained (% w/v) $\text{FeSO}_4 \cdot 7\text{H}_2\text{O}$, 0.1; $\text{CuSO}_4 \cdot 5\text{H}_2\text{O}$, 0.015; $\text{ZnSO}_4 \cdot 7\text{H}_2\text{O}$, 0.161; and $\text{MnSO}_4 \cdot 7\text{H}_2\text{O}$, 0.008.

The three types of AO-UBERs were operated under different voltage application modes (0.5, 0.8 and 1.2 V). A reactor was operated intermittently in the regime “one day ON/one day OFF” (‘R1’ hereafter). The continuous voltage application modes (‘R2’ hereafter) were compared with the control system (‘R3’ hereafter) that was not exposed to voltage.

In the initial stage, the three reactors were fed synthetic CAP wastewater with a 24 h HRT. When all reactors exhibited the same CAP removal efficiency, a voltage of 1.2 V, as indicated in our previous study (Ailijiang et al., 2016), was applied to R1 and R2. The aerobic biodegradation of phenol was enhanced by electrical stimulation. Based on the removal of CAP, the HRT was increased to 36 h. The applied voltage was gradually reduced from 1.2 V to 0.5 V to reduce energy consumption.

2.4 Analytical methods

2.4.1 Chemicals and analytical methods

CAP ($\text{C}_{11}\text{H}_{12}\text{Cl}_2\text{N}_2\text{O}_5$, $M_w = 323.13$, 98% purity) was

purchased from Shanghai Yuanye Biotechnology Co., Ltd. (China). CFNs and GACs were purchased from Beijing Jinglongte Carbon Technology Co., Ltd. (China) and the Lvlin activated carbon plant (Henan, China), respectively. Other chemicals, including HCl, NH_4Cl , $\text{K}_2\text{HPO}_4 \cdot 3\text{H}_2\text{O}$, $\text{C}_6\text{H}_{12}\text{O}_6$ and KCl were purchased from Tianjin Shengao Chemical Reagent Co., Ltd. (China) and were of analytical grade. High-performance liquid chromatography (HPLC)-grade methanol and acetonitrile were purchased from Sigma-Aldrich (St. Louis, MO, USA).

CAP degradation products were identified using HPLC-tandem mass spectrometry (MS/MS) (ion trap) (Thermo Finnigan LCQ Deca XP Max LC/MS, Germany). The electrospray ion source with positive and negative modes and mass scanning varied from 50 to 500 m/z. The substance was qualitatively analyzed using the primary mass spectrum in the full-scan mode. The chromatographic column was C18 (4.6 mm × 150 mm, 5 μm), with methanol/water (55:45, v/v) as the mobile phase at a flow rate of 0.8 mL/min; the detection temperature was 30°C and the injection volume was 10 μL .

The COD concentrations of the influent and effluent samples were quantified using a potassium dichromate titration. Dissolved oxygen (DO) concentrations and pH values in the effluent were measured once daily using a DO meter and a pH meter (JPB-607A and PHBJ-260, Shanghai INESA Scientific Instrument, China).

2.4.2 Microbial community analysis

Eight samples were collected at the end of the long-term experiment and seed sludge, tagged as IAe and IAn (from the anode and cathode of R1 reactor), CAe and CAn (from the anode and cathode of R2 reactor), ZAe and ZAn (from the aerobic and anaerobic zones of R3 reactor) along with RAe and RAn (from the aerobic and anaerobic

seed sludge). DNA was extracted from the samples using a Fast-DNA Spin Kit for Soil (MP Biomedicals, Santa Ana, CA, USA) following the manufacturer's instructions. For high-throughput sequencing, 16S rRNA genes were amplified using the primers 515F (5'-GTGCCAGCM-GCCGCGTAA-3') and 806R (5'-GGACTACHVGGGT-WTCTAAT-3'), targeting the V3–V4 region of the 16S rRNA gene. Sequencing was performed using an Illumina MiSeq platform (Biomark Biotechnology Co., Ltd., China).

We used Trimmomatic v0.33, Cutadapt 1.9.1, FLASH v1.2.7 and UCHIME v4.2 for filtering, denoising, splicing and removing chimeras to obtain the final effective data (effective reads). The Usearch software was used to cluster reads at a similarity level of 97.0% to obtain operational taxonomic units (OTUs). These were used for species annotation and abundance analysis to determine the composition of species in the sample. This experiment includes alpha diversity analysis, which mainly reflects the degree of abundance of community bacteria in a single sample, using the Shannon-Weiner and Chao index.

Alpha diversity expresses the species abundance (richness) and species diversity of a single sample, where the Chao1 and ACE indices reflect species abundance (e.g., the number of species). Shannon and Simpson indices were used to measure species diversity and were affected by the abundance of species in the sample community and the evenness of species (community evenness) (Grice et al., 2009). Gotaq qPCR Master Mix (Promega, Madison, WI, USA) was used and the composition of the quantitative polymerase chain reaction (qPCR) mixture was the same as that used in a previous study.

2.5 Statistical analysis

Statistical analyses were performed using SPSS (version 25.0, SPSS Inc. Chicago, IL, USA). One-way ANOVA

and Fisher's LSD test at a 0.05 probability level were used to evaluate the significance of differences in CAP removal rates among the three treatments.

3 Results and discussion

3.1 Effect of electrical stimulation on attenuation of CAP and COD

The overall performance of the AO-UBER on the CAP and the last five days (days 36–40) of COD removal is shown in Fig. 2. The electrical enhancement effect varied with different voltages (0.5, 0.8 and 1.2 V), HRTs (24 and 36 h) and voltage application modes (intermittent and continuous) in Fig. 2A. At stage 1, the CAP removal efficiencies of the three reactors exhibited the same trend: $53.2\% \pm 0.9\%$ (R1), $53.2\% \pm 0.7\%$ (R2) and $53.1\% \pm 0.6\%$ (R3), at an influent concentration of 10.8 ± 0.3 mg/L during the initial 6 d with an HRT of 24 h.

Starting on day 7, a voltage of 1.2 V was applied to R1 and R2 in stage 2, following the methodology of our previous study (Ailijiang et al., 2016) and the HRT was maintained at 24 h. The CAP removal efficiencies in R1 and R2 rapidly decreased to $48.4\% \pm 2.2\%$ and $44.6\% \pm 5.1\%$, respectively. This decrease appeared to be driven by the rupture of the cytoplasm of some bacteria at higher voltages which inhibited their metabolic activity (Zhang et al., 2014). This may have led to a decrease in CAP metabolism by the bacteria in the reactor, which worsened its attenuation.

Starting on day 13, bacterial activity in R1 and R2 was restored by reducing the applied voltage to 0.8 V. After 6 d of cultivation, the treatment efficiencies of R1 and R2 were restored to $55.2\% \pm 2.7\%$ and $53.9\% \pm 4.0\%$, respectively. These were similar to that of R3 ($53.8\% \pm 1.0\%$). This indicated that the bacterial activity was temporarily inhibited under short-term high-voltage conditions

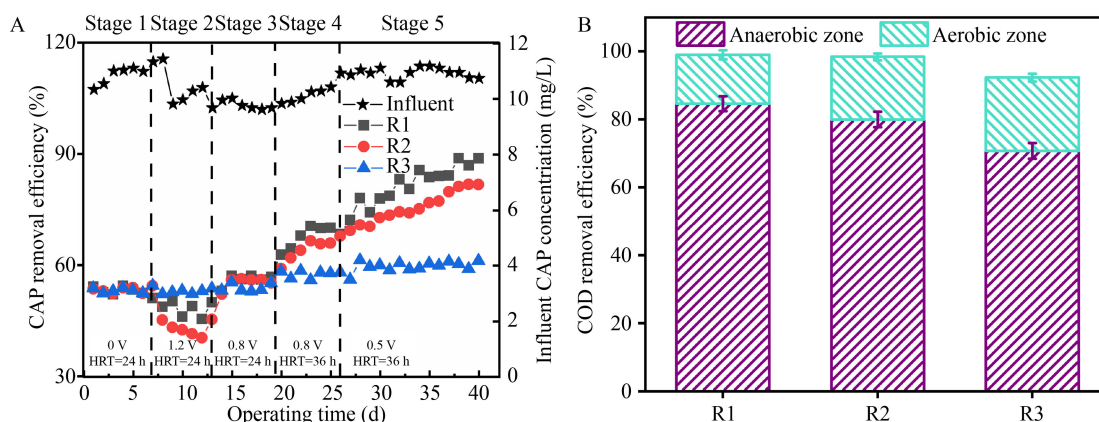


Fig. 2 (A) CAP removal performances of AO-UBERs during the long-term operation and (B) COD removal performances of AO-UBERs during stage 5.

($p < 0.05$). Moreover, high voltages can inhibit microbial enzyme activity, ultimately reducing the rate of microbial metabolism (Zhang et al., 2014).

Starting on day 20, the HRT was increased from 24 to 36 h to increase the contact time between the bacteria and CAP to better observe the effect of electrical stimulation. The CAP removal efficiencies in R1 and R2 increased by 12.4% and 10.0%, respectively and the treatment efficiency of R3 did not significantly improve. This finding showed that CAP biodegradation was improved through electrical stimulation, which was mainly attributed to the enrichment of electroactive bacteria and the improvement of microbial activity (Logan et al., 2019).

From day 26, the applied voltage was reduced from 0.8 to 0.5 V with a HRT of 36 h to reduce the energy consumption required for the operation. The CAP removal rates in R1 and R2 were 21.5% and 15.6% greater than that in R3 ($p < 0.05$), respectively.

Notably, COD removal efficiency is one of the key indicators for measuring the effect of the reactor on sewage treatment. After the reactor had been operated for 35 days, the COD of the effluent was measured. The COD removal efficiencies of the three reactors over the last 5 days are shown in Fig. 2(B). The COD was nearly completely degraded in the last 5 d in R1 ($99.0\% \pm 0.9\%$) and R2 ($98.4\% \pm 2.0\%$), which was significantly greater than the COD degradation in R3 ($92.3\% \pm 2.2\%$). The COD removal efficiencies in the anaerobic zones of R1, R2 and R3 were $84.6\% \pm 2.2\%$, $79.9\% \pm 2.3\%$ and $70.7\% \pm 2.3\%$, respectively. Applying an appropriate voltage could improve the COD removal capacity. The intermittent electrical stimulation mode had superior performance to the continuous mode ($p < 0.05$). It may be verified that the metabolic activity of the microbial community is improved after the voltage is applied (Ailijiang et al., 2021b) and intermittent application of voltage is conducive to the formation of the co-metabolic community of bacteria during the long-term domestication process, thereby improving the COD removal efficiency. By reducing the concentration of CAP in R1 and R2, the applied voltage may explain why the inhibition of the microbial metabolism was diminished. The COD removal efficiencies of the aerobic zones of R1, R2 and R3 were $14.4\% \pm 1.3\%$, $18.4\% \pm 1.0\%$ and $21.6\% \pm 1.1\%$, respectively, which were opposite to those in the anaerobic zone. This finding can be explained by glucose being completely degraded in the electric reactor, leaving less degradable substances in the aerobic zone. Consequently, the COD degradation efficiency of the electric reactor was less than that of the control reactor.

This result indicated that when the applied voltage decreased to 0.5 V, electrical stimulation significantly promoted CAP and COD biodegradation, especially in the intermittent voltage application mode. Our results also agree with those of a previous study (Cao et al., 2016), that reported that intermittent electrical stimulation mode

was superior to continuous mode. A possible explanation for this phenomenon is that electrical stimulation weakens the antibacterial activity during the decomposition of CAP (Liang et al., 2019). Moreover, most electroactive bacteria are enriched in the intermittent electrical stimulation mode, resulting in a better treatment effect in the intermittent voltage application mode than in the continuous electrical stimulation mode (Zhang et al., 2019; Ailijiang et al., 2021b).

3.2 Contribution of anodic and cathodic chambers in the removal of CAP

Figure 3 shows the CAP degradation performance of the aerobic and anaerobic chambers of the AO-UBERs at different HRTs and voltages. The anaerobic chamber mainly contributed to CAP biodegradation for the duration of the experiment in all reactors, which was attributed to chloro or nitro substituents succumbing to electrophilic attack more readily under anaerobic conditions (Jiang et al., 2021). The aerobic chamber exhibited almost no CAP degradation, which is consistent with the electron-withdrawing properties of the nitro and chlorine atomic groups in CAP. These groups are resistant to microbial oxidative degradation (Lin et al., 2011).

The treatment efficiency of R1, R2 and R3 in the anaerobic chamber for CAP was improved by 12.5%, 9.98% and 3.65%, respectively, in stage 4. The increased HRT may be responsible for this phenomenon. It prolonged the exposure time of CAP in the biofilm, which enhanced the CAP degradation efficiency. Remarkably, the effect of electrical stimulation intensification was manifested after prolonged HRT, seemingly caused by the elevated interaction time between electrodes and biofilms, additionally, the reduced inhibition pressure of CAP on bacteria (Wang et al., 2022).

From day 26, the treatment efficiency of CAP by R1 and R2 reached $80.2\% \pm 6.0\%$ and $74.1\% \pm 4.6\%$, respectively, in the anaerobic chamber; however, the efficiency of CAP decomposition by R3 in the anaerobic chamber was only $58.5\% \pm 1.4\%$. These results are consistent with previous findings (Liang et al., 2016). These studies concluded that the cathode chamber accelerated the CAP biodegradation rates. Electrochemical and morphological analyses showed that some functional bacteria that degraded CAP were enriched in the biocathode, thereby improving the CAP degradation efficiency. The biocathode enhances the dechlorination and nitroreduction procedures as an electron donor (Zhang et al., 2019; Ailijiang et al., 2021b). Therefore, the low-biototoxicity products migrated into the anode chamber and experienced oxidative decomposition.

3.3 Effect of electrical stimulation on microbial communities

Our results indicate that electrical stimulation has a

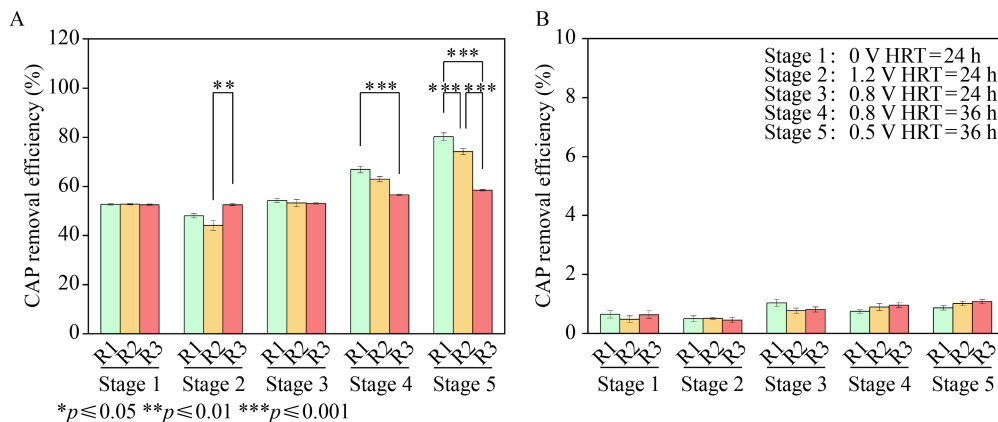


Fig. 3 CAP removal performance in the anaerobic zones (A) and aerobic zones (B) of AO-UBERs under different HRTs and applied voltages.

significant effect on the anaerobic and aerobic biological treatment of CAP. Thus, we argue that the biological community structures of anaerobic and aerobic bacteria may differ under different electrical stimulation modes. To evaluate this, we analyzed the 16S rRNA gene high-throughput sequencing data of the microbial community structure of GAC and CFN biofilms under aerobic and anaerobic conditions in the three reactors, after 40 d of operation. In addition, we compared the obtained sequence information with existing databases. The classification of the OTUs in each sample was also compared. We further discussed some key points at the phylum and genus levels.

3.3.1 Quantification of total bacteria

In our previous studies, biofilms were the main contributors to the degradation of contaminants and the contribution of suspended microorganisms to pollutant degradation was negligible in AO-UBER (Ailijiang et al., 2016; Ailijiang et al., 2021a; 2021b). Therefore, the biomass in the biofilms attached to CFNs and GAC was collected to quantify the total bacterial biomass in the six chambers. This step was performed according to a previous experimental qPCR analysis method to quantify the total bacterial count (Ailijiang et al., 2016). Table 1 shows the \log_{10} (copies/one CFN or g GAC) of the six bacterial samples, which were 10.11, 9.45, 10.05, 9.50, 10.02 and 9.63 for IAn, IAe, CAn, CAe, ZAn and Z Ae, respectively. Overall, there was no significant difference in biomass between the aerobic and anaerobic chambers in the three reactors after 40 d of operation. This finding was consistent with the results of our preliminary study (Ailijiang et al., 2021b). Moreover, our results suggest that the total number of bacteria does not have a distinct effect on electrical stimulation. The enhanced CAP degradation rates in electrically stimulated reactors were not affected by the total number of bacteria.

3.3.2 Microbiological diversity analysis

As shown in Supplementary Material (Fig. S2 and Table S2), the coverage values were all > 0.999 and the rarefaction curve started slowing at > 27500 in addition to the measured sequences. This indicated that the microbial diversity sequencing data in this experiment were highly reliable and that the biological sequencing data were valid. Table 1 shows the ACE, Chao1, Simpson and Shannon indices of the eight microbiological samples, which are widely used to assess the diversity and abundance of microbial communities.

The ACE of CAn and IAn (686.4 and 692.9) was less than that of ZAn (697.6), while the Simpson (0.95 and 0.94) and Shannon indices (5.3 and 5.7) of the CAn and the IAn were greater than those of ZAn (0.92 and 5.3). Interestingly, these results indicated that the abundance of bacteria decreased, whereas their diversity increased, further suggesting that microbes on the cathode surface became more abundant under electrical stimulation. Ecological stability increases when biodiversity is high because it allows microbial communities to resist adverse external conditions (Zhang et al., 2013). Appropriate electrical stimulation can improve the stability of microbial community structures. This enhances the stability of the microbial community structure in toxic environments (Wang et al., 2022). In particular, the abundance index of IAn was slightly higher than that of CAn and the diversity index was lower than that of CAn. Cathode biofilms can provide electrons for the reduction of organic compounds. Thus, for CAP-degrading bacteria, it was beneficial to enrich the cathode and replace other bacteria, reducing the bacterial diversity in the cathode biofilms.

In the aerobic zone, the ACE (682.6) and Chao1 (691.3) of IAe were less than those of CAe (709.9, 709.6) and Z Ae (705.3, 705.4), which may be due to the R1 anaerobic zone having a higher COD degradation efficiency, resulting in a lower COD concentration in the aerobic zone. In brief, this was not conducive to bacterial

Table 1 Microbial community diversity, abundance index and Q-PCR quantification of microbial samples

Sample ID	ACE ^{a)}	Chao1 ^{a)}	Simpson ^{b)}	Shannon ^{b)}	log ₁₀ (copies/ one CFN or g GAC)
IAn	692.9	700.3	0.94	5.7	10.11
CAn	686.4	699.2	0.95	5.9	10.05
ZAn	697.6	698.2	0.92	5.3	10.02
IAe	682.6	691.3	0.94	5.7	9.45
CAe	709.9	709.6	0.95	5.8	9.50
ZAe	705.3	705.4	0.94	6.1	9.63
RAn	661.0	671.2	0.89	4.9	/
RAe	692.2	698.5	0.96	6.1	/

Notes: a) Abundance index of the microbial community. A higher number represents greater abundance. b) Diversity index. A higher number indicates greater diversity.

enrichment. Interestingly, the Shannon index of ZAe (6.1) was greater than those of CAe (5.8) and IAe (5.7). The low microbial metabolism can partly explain this in the anaerobic zone of R3, which provides a wide variety of metabolites to its aerobic zone, thereby maintaining high biodiversity. This phenomenon was inconsistent with the changes in the abundance and diversity of bacteria in the anaerobic zone. This phenomenon may be driven by the difference in the CAP and COD concentrations in the influent water of the aerobic zone.

3.3.3 Analysis of microbial community structure

After filtering the chimera from the eight samples, we detected > 69500 effective sequences, with an average length of 420–422 bps. At a similarity level of 97%, there were 667, 667, 671, 636, 659, 680, 696 and 677 OTUs for IAn, CAn, ZAn, RAn, IAe, CAe, ZAe and RAe, respectively.

The composition and relative abundance of microbial communities at the phylum level in the three AO-UBERS are shown in Fig. 4(A). During the operation of the reactors, the community structure in all reactors. We changed compared to that of the inoculated sludge. The bacterial community structures of the aerobic and anaerobic biofilms were identified at the phylum level in all reactors. Our study found that *Proteobacteria* (29.7%–39.2%), *Bacteroidetes* (16.6%–40.4%) and *Firmicutes* (6.56%–27.5%) were the dominant phyla in all samples. At the phylum level, this community structure is similar to that reported in previous studies (Logan et al., 2019; Ailijiang et al., 2021b).

The relative abundances of *Proteobacteria* (39.2%), *Bacteroidetes* (21.5%), *Firmicutes* (27.5%) and *Cyanobacteria* (3.37%) in IAn were greater than those in the CAn (34.1%, 18.7%, 27.1% and 2.21%) and ZAn (35.4%, 16.6%, 22.8% and 1.07%). *Patescibacteria* (5.26%) in IAn were slightly lower than those in CAn (8.43%) and ZAn (9.31%), whereas *Verrucomicrobia* had nearly

disappeared. This finding indicates that *Verrucomicrobia* may not participate in the CAP degradation in this system or that its growth and metabolism were inhibited by the CAP. Interestingly, *Fusobacteria* were significantly greater in both the cathode and anode chambers of R2 (12.3%–14.5%) than in R1 (1.12%–7.43%) and R3 (2.28%–6.29%).

Among aerobic bacteria, the main bacterial phyla were *Proteobacteria*, *Bacteroidetes*, *Firmicutes*, *Patescibacteria*, *Fusobacteria*, and *Verrucomicrobia*. In the biofilms of ZAe, *Bacteroidetes* (20.4%), *Fusobacteria* (2.28%) and *Verrucomicrobia* (4.69%) were lower than the IAe (40.4%, 7.43% and 7.39%) and CAe (28.8%, 14.5% and 15.2%, respectively). This finding indicates that electrical stimulation selectively enriched specific bacteria in the cathode and anode compartments of AO-UBERS. However, there were no significant differences in the bacterial community structure between the aerobic and anaerobic zones. This indicates that 35 days of electrical stimulation did not alter the community structure at the phylum level.

To further explore the differences in specific bacteria between the reactors, the 41 most abundant bacteria were analyzed at the genus level. To this end, a heat map was constructed and clustered. Figure 4(B) shows that the cathode and anode chambers of R1 and R2 were clustered together. Moreover, the clustering results suggest that electrical stimulation affected the bacterial community structure.

The dominant genera in anaerobic biofilm samples were found to be *Cetobacterium*, *Desulfovibrio*, *Janthinobacterium*, *Lactococcus*, *Megasphaera*, and *Selenomonas*, with relative abundances of 0.78%–12.0%, 4.84%–7.60%, 1.94%–5.23%, 3.80%–5.64%, 3.87%–5.26% and 3.03%–4.69%, respectively. *Acidovorax*, *Cetobacterium*, *Fibrella*, *Prostheco bacter*, *Emticicia*, *Reyranelia*, and *Zoogloea*, with relative abundances of 0.89%–8.49%, 1.96%–14.2%, 4.53%–10.1%, 2.77%–8.28%, 0.16%–18.9%, 1.55%–5.28% and 0.10%–5.53%, respectively, were dominant in the anaerobic biofilm samples. These results implied that the functional microbes in the biofilms, involved in the biodegradation of CAP and its metabolites, were enriched during long-term operation.

For instance, *Bacteroides* (1.36%–1.46%), *Caproiciproducens* (1.06%–2.64%), *Cloacibacterium* (0.61%–1.13%), *Flavobacterium* (0.32%–0.80%), *Janthinobacterium* (4.50%–5.23%), *Lactococcus* (4.96%–5.64%), *Megasphaera* (5.02%–5.26%), *Pantoea* (0.75%–1.52%), and *Pseudomonas* (0.75%–1.65%) were enriched in the R1 and R2 cathode chambers. *Pseudomonas* and *Flavobacterium* are important denitrifying bacteria (Cao et al., 2022). There is evidence that *Cloacibacterium* is an electroactive bacterium capable of promoting the transformation of electrons within benzene rings in biofilms and it is also capable of degrading 2,4-dichlorophenol (Hassan et al., 2018; Zheng et al., 2019). *Caproiciproducens* and *Megasphaera* are

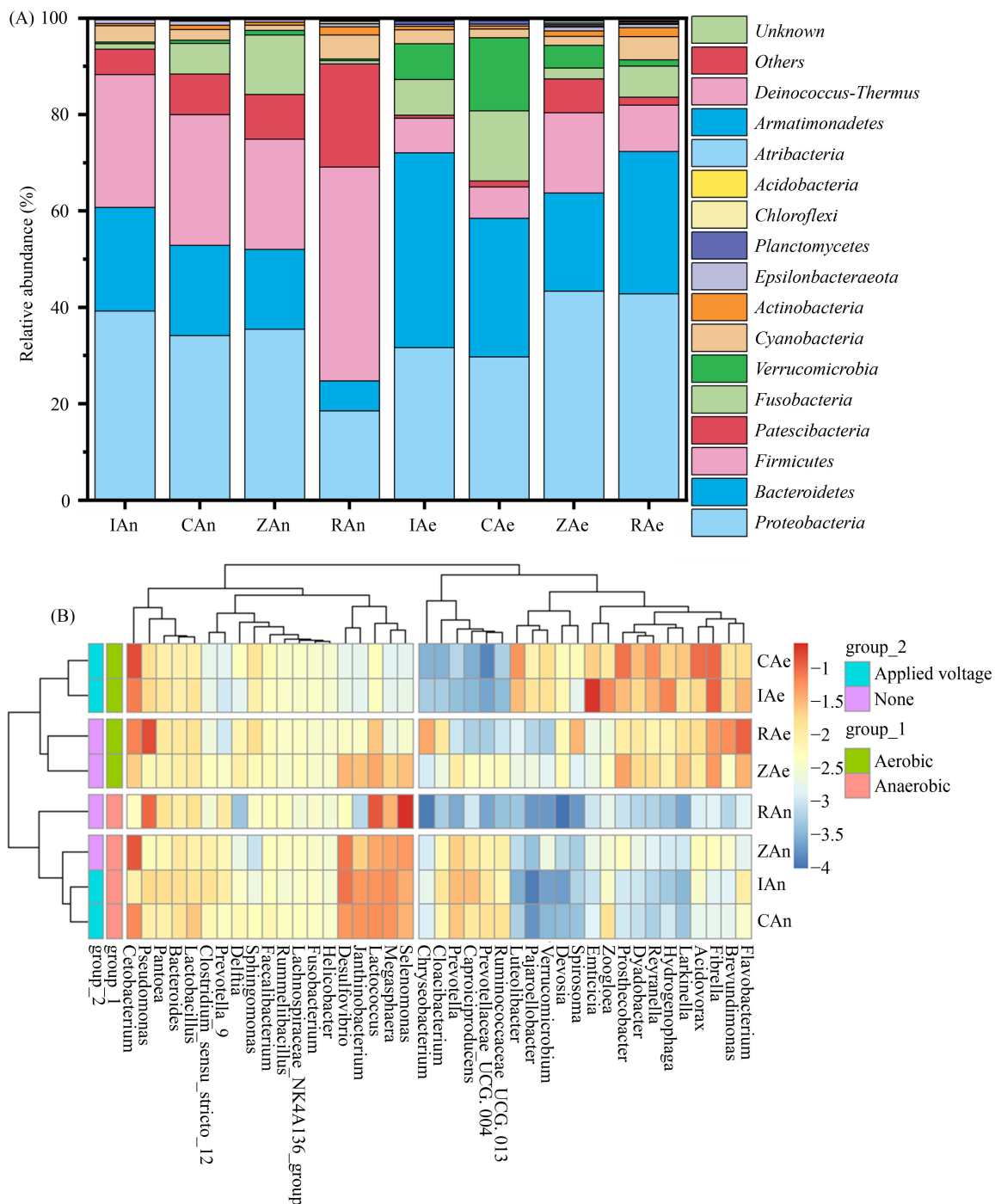


Fig. 4 Relative abundance of bacterial community composition in (A) eight samples at the phylum level and (B) the heatmap of the most abundant genera. Only the most populous 41 genera were used to build the heat map, and the color intensity showed the relative abundance of the genera in a sample. RAn and RAe were from anaerobic and aerobic seed sludges. IAn, CAn and ZAn biofilm samples were from the anaerobic zones of R1, R2 and R3; IAe, CAe and ZAE biofilm samples from the aerobic zones of R1, R2 and R3.

both crucial fermenting and hydrogen-producing bacterial genera (Ta et al., 2020; Kim et al., 2022), and their enrichment at the cathode opens a window for more efficient use of electrons released from the cathode. It is also widely acknowledged that *Janthinobacterium* can remove NH_4^+ and possess a range of denitrifying enzymes, capable of reducing nitrate into nitric oxide

(Cho et al., 2017).

Furthermore, the relative abundances of *Acidovorax* (1.68%–8.49%), *Cetobacterium* (7.03%–14.2%), *Dyadobacter* (1.68%–2.61%), *Luteolibacter* (2.66%–4.93%), *Hydrogenophaga* (1.79%–6.20%), *Reyranelia* (3.10%–5.28%), and *Zoogloea* (1.03%–5.83%) were greater than ZAE (0.89%, 1.96%, 1.66%, 0.18%, 0.96%, 1.55% and

0.40%) among the aerobic biofilm samples following electrical stimulation. Previous studies have demonstrated that *Acidovorax*, *Cetobacterium*, and *Dyadobacter* can promote organochlorine degradation (Monferrán et al., 2005; Gregory et al., 2015; Hassan et al., 2018). *Hydrogenophaga* and *Luteolibacter* species are considered degraders of refractory organic contaminants (Cébron et al., 2015; Zheng et al., 2019) and *Luteolibacter* is thought to be capable of hydrolyzing p-nitrophenyl (Nagao et al., 2017).

Desulfovibrio was dominant in the IAn and it has been shown that *Desulfovibrio* can reduce CAP to the corresponding aromatic amines (Liang et al., 2016). Additionally, *Megasphaera* was enriched in all cathode chamber biofilms and had the highest abundance in IAn. *Megasphaera* is a strictly anaerobic ruminant soluble substrate fermenter that uses polymer hydrolysis products provided by other bacteria as a source of nutrients (Marounek et al., 1989). This explains the enrichment of *Megasphaera* in all cathodic chambers. Simultaneously, the species of *Janthinobacterium* have a series of denitrifying enzymes, which can finally reduce nitrate to nitric oxide (Cho et al., 2017), indicating that *Janthinobacterium* can remove nitrate-nitrogen from the metabolites of other species. *Janthinobacterium* was more abundant in the cathode chambers of the IAn and ZAn. *Emticicia* and *Hydrogenophaga* were able to reduce nitrate and nitrite in the anode chamber and both had a significant growth advantage in IAn. This finding indicates that the bacteria in the IAn reduced the CAP and subsequently provided nitrate and nitrite through upflow. Specifically, the amounts of nitrate and nitrite provided by the cathodic chamber bacteria of IAn after the reduction of the CAP through upflow were higher. This explains the higher efficiency of the CAP treatment with the IAn. The functions of the corresponding genera allow the assumption that during reactor operation, cathode chamber bacteria such as *Desulfovibrio* metabolized and reduced the CAP. *Megasphaera* and *Janthinobacterium* then treated CAP products to produce a certain amount of nitrate and nitrite, which allowed *Emticicia* and *Hydrogenophaga* to reduce in the anode chamber resulting in better enrichment. *Emticicia* and *Hydrogenophaga*, which can reduce nitrate and nitrite, respectively, were more enriched in the anode chamber. We surmised that the supply of electrons by the electrodes in the cathodic chamber enhanced the ability of the bacteria in the cathodic chamber to reduce the CAP, and that the CAP degradation efficiency was maximally enhanced in the intermittent mode.

3.4 CAP reduction pathways

In AO-UBERs, CAP decomposition is a bioelectrochemical process in which complex intermediates are formed during the CAP degradation. HPLC-MS/MS detected the

products formed during the CAP degradation process. The substitute name, chemical name, molecular formulas and M/Z ratios of the possible compounds are listed in the Supplementary Material (Fig. S3 and Table S3). The principal metabolic pathways of CAP and its metabolites in the AO-UBERs are shown in Fig. 5. Three principal processes occur in the anaerobic zone: (1) hydrolysis of the peptide bond within CAP to produce CAP-hydrolysed amino products (CAP-(C₂H₂Cl₂NO)) and dichloroacetic acid. Toward the end of the synthesis process, (CAP-(C₂H₂Cl₂NO)) undergoes nitro-ammoniation to yield 4-hydroxyaminobenzoic acid, which ultimately loses its biotoxicity. (2) Initially, CAP is acetylated to produce CAP-acetyl. Subsequently, it undergoes a nitro-ammoniation reaction to produce AMCl₂-acetyl with nitro-reducing bacteria (*Janthinobacterium*, *Pseudomonas*, *Flavobacterium*, and *Desulfovibrio*) which are enriched in voltage application reactors. It undergoes a two-step dechlorination reaction to produce AM-acetyl with dechlorination bacteria (*Cloacibacterium*) that are enriched in voltage application reactors, during which some molecules undergo hydrolysis and lose chlorine atoms or undergo dechlorination to become non-toxic. (3) CAP undergoes nitroammoniation to yield AMCl₂ and a two-step dechlorination reaction to produce AM with nitro-reducing and dechlorination bacteria. Ultimately, CAP reaches the aerobic zone and is completely degraded. Following the elimination of toxicity from the anaerobic area, the degradation products were further oxidized in the aerobic zone into carbon dioxide and water. Functional microorganisms involved in metabolic processes (2) and (3) are enriched in the biocathode, which effectively reduces the antibacterial activity of CAP (Liang et al., 2013). By analyzing the CAP metabolic process, it can be inferred that EBT mainly enhances CAP degradation by enriching functional microorganisms to accelerate the critical CAP degradation process. However, it did not alter the CAP metabolic pathways.

4 Conclusions

In this study, AO-UBER improved the decomposition efficiency of CAP under the application of intermittent voltage and the promoting effect of exoelectrogenic biofilms was reflected under the appropriate HRT. Both electrical stimulation modes shifted the microbial community structure, enriched the electroactive microorganisms and promoted the degradation of antibiotics. In addition, the electroactive biofilm can maintain high treatment efficiency when the voltage is reduced after the electric strengthening effect occurs. AO-UBER offers new ideas for the treatment of antibiotics in agriculture, medical wastewater and WWTPs. In future studies, the AO-UBER may further demonstrate its potential by simulating wastewater containing multiple antibiotics. In addition,

- with exposing to silver nanoparticles. *Journal of Hazardous Materials*, 432: 128642
- Cao Z, Zhang M, Zhang J, Zhang H (2016). Impact of continuous and intermittent supply of electric assistance on high-strength 2,4-dichlorophenol (2,4-DCP) degradation in electro-microbial system. *Bioresource Technology*, 212: 138–143
- Cébron A, Beguiristain T, Bongoua-Devisme J, Denonfoux J, Faure P, Lorgeoux C, Ouvrard S, Parisot N, Peyret P, Leyval C (2015). Impact of clay mineral, wood sawdust or root organic matter on the bacterial and fungal community structures in two aged PAH-contaminated soils. *Environmental Science and Pollution Research International*, 22(18): 13724–13738
- Cho Y J, Jung Y J, Hong S G, Kim O S (2017). Complete genome sequence of a psychrotolerant denitrifying bacterium, *Janthinobacterium svalbardensis* PAMC 27463. *Genome Announcements*, 5(46): e01178–17
- Gregory S J, Anderson C W N, Camps-Arbestain M, Biggs P J, Ganley A R D, O'Sullivan J M, McManus M T (2015). Biochar in co-contaminated soil manipulates arsenic solubility and microbiological community structure, and promotes organochlorine degradation. *PLoS One*, 10(4): e0125393
- Grice E A, Kong H H, Conlan S, Deming C B, Davis J, Young A C, Bouffard G G, Blakesley R W, Murray P R, Green E D, Turner M L, Segre J A (2009). Topographical and temporal diversity of the human skin microbiome. *Science*, 324(5931): 1190–1192
- Hassan H, Jin B, Donner E, Vasileiadis S, Saint C, Dai S (2018). Microbial community and bioelectrochemical activities in MFC for degrading phenol and producing electricity: Microbial consortia could make differences. *Chemical Engineering Journal*, 332: 647–657
- Jiang X, Shen J, Han Y, Lou S, Han W, Sun X, Li J, Mu Y, Wang L (2016). Efficient nitro reduction and dechlorination of 2,4-dinitrochlorobenzene through the integration of bioelectrochemical system into upflow anaerobic sludge blanket: A comprehensive study. *Water Research*, 88: 257–265
- Jiang X B, Chen D, Mu Y, Pant D, Cheng H Y, Shen J Y (2021). Electricity-stimulated anaerobic system (ESAS) for enhanced energy recovery and pollutant removal: A critical review. *Chemical Engineering Journal*, 411: 128548
- Kim B C, Moon C, Choi Y, Nam K (2022). Long-term stability of high-n-caproate specificity-ensuring anaerobic membrane bioreactors: controlling microbial competitions through feeding strategies. *ACS Sustainable Chemistry & Engineering*, 10(4): 1595–1604
- Liang B, Cheng H Y, Kong D Y, Gao S H, Sun F, Cui D, Kong F Y, Zhou A J, Liu W Z, Ren N Q, Wu W M, Wang A J, Lee D J (2013). Accelerated reduction of chlorinated nitroaromatic antibiotic chloramphenicol by biocathode. *Environmental Science & Technology*, 47(10): 5353–5361
- Liang B, Kong D, Ma J, Wen C, Yuan T, Lee D J, Zhou J, Wang A (2016). Low temperature acclimation with electrical stimulation enhance the biocathode functioning stability for antibiotics detoxification. *Water Research*, 100: 157–168
- Liang B, Ma J, Cai W, Li Z, Liu W, Qi M, Zhao Y, Ma X, Deng Y, Wang A, Zhou J (2019). Response of chloramphenicol-reducing biocathode resistome to continuous electrical stimulation. *Water Research*, 148: 398–406
- Lin H Z, Zhu L A, Xu X Y, Zang L L, Kong Y (2011). Reductive transformation and dechlorination of chloronitrobenzenes in UASB reactor enhanced with zero-valent iron addition. *Journal of Chemical Technology and Biotechnology (Oxford, Oxfordshire)*, 86(2): 290–298
- Logan B E, Rabaey K (2012). Conversion of wastes into bioelectricity and chemicals by using microbial electrochemical technologies. *Science*, 337(6095): 686–690
- Logan B E, Rossi R, Ragab A, Saikaly P E (2019). Electroactive microorganisms in bioelectrochemical systems. *Nature Reviews. Microbiology*, 17(5): 307–319
- Marounek M, Fliegerova K, Bartos S (1989). Metabolism and some characteristics of ruminal strains of *Megasphaera elsdenii*. *Applied and Environmental Microbiology*, 55(6): 1570–1573
- Monferrán M V, Echenique J R, Wunderlin D A (2005). Degradation of chlorobenzenes by a strain of *Acidovorax avenae* isolated from a polluted aquifer. *Chemosphere*, 61(1): 98–106
- Nagao T, Kumabe A, Komatsu F, Yagi H, Suzuki H, Ohshiro T (2017). Gene identification and characterization of fucoidan deacetylase for potential application to fucoidan degradation and diversification. *Journal of Bioscience and Bioengineering*, 124(3): 277–282
- Ta D T, Lin C Y, Ta T M, Chu C Y (2020). Biohythane production via single-stage fermentation using gel-entrapped anaerobic microorganisms: Effect of hydraulic retention time. *Bioresource Technology*, 317: 123986
- Tang H, Wang J Q, Zhang S, Pang H W, Wang X X, Chen Z S, Li M, Song G, Qiu M Q, Yu S J (2021). Recent advances in nanoscale zero-valent iron-based materials: Characteristics, environmental remediation and challenges. *Journal of Cleaner Production*, 319: 128641
- Wang S, Xu M, Jin B, Wunsch U J, Su Y, Zhang Y (2022). Electrochemical and microbiological response of exoelectrogenic biofilm to polyethylene microplastics in water. *Water Research*, 211: 118046
- Wu Q, Chang J L, Yan X, Ailijiang N, Fan Q X, Wang S H, Liang P, Zhang X Y, Huang X (2016). Electrical stimulation enhanced denitrification of nitrite-dependent anaerobic methane-oxidizing bacteria. *Biochemical Engineering Journal*, 106: 125–128
- Xiong R, Wei X, Jiang W, Lu Z, Tang Q, Chen Y, Liu Z, Kang J, Ye Y, Liu D (2022). Photodegradation of chloramphenicol in micro-polluted water using a circulatory thin-layer inclined plate reactor. *Chemosphere*, 291(Pt 2): 132883
- Xue Y, Wang Z H, Bush R, Yang F, Yuan R X, Liu J S, Smith N, Huang M H, Dharmarajan R, Annamalai P (2021). Resistance of alkyl chloride on chloramphenicol to oxidative degradation by sulfate radicals: Kinetics and mechanism. *Chemical Engineering Journal*, 415: 129041
- Yang Y J, Xu L J, Wang J L (2021). An enhancement of singlet oxygen generation from dissolved oxygen activated by three-dimensional graphene wrapped nZVI-doped amorphous Al species for chloramphenicol removal in the Fenton-like system. *Chemical Engineering Journal*, 425: 131497
- Zhang J, Zhang Y, Quan X, Chen S (2013). Effects of ferric iron on the anaerobic treatment and microbial biodiversity in a coupled microbial electrolysis cell (MEC) —anaerobic reactor. *Water Research*, 47(15): 5719–5728

- Zhang J L, Hu J, Zhang T T, Cao Z P (2019). Improvement of 2,4-dichlorophenol degradation and analysis of functional bacteria in anaerobic microbial system enhanced with electric assistance. *Bioresource Technology Reports*, 5: 80–85
- Zhang X Q, Feng H J, Shan D, Shentu J, Wang M Z, Yin J, Shen D S, Huang B C, Ding Y C (2014). The effect of electricity on 2-fluoroaniline removal in a bioelectrochemically assisted microbial system (BEAMS). *Electrochimica Acta*, 135: 439–446
- Zhao R, Feng J, Huang J, Li X, Li B (2021). Responses of microbial community and antibiotic resistance genes to the selection pressures of ampicillin, cephalexin and chloramphenicol in activated sludge reactors. *Science of the Total Environment*, 755(Pt 2): 142632
- Zheng M Q, Xu C Y, Zhong D, Han Y X, Zhang Z W, Zhu H, Han H J (2019). Synergistic degradation on aromatic cyclic organics of coal pyrolysis wastewater by lignite activated coke-active sludge process. *Chemical Engineering Journal*, 364: 410–419